Available online at www.sciencedirect.com

ScienceDirect

Procedia Engineering 120 (2015) 711 – 716

Procedia Engineering

www.elsevier.com/locate/procedia

EUROSENSORS 2015

# ZnO nanostructures to detect low concentrations of indoor pollutants

J. Gonzalez-Chavarri[1,2], I. Castro-Hurtado[1,2], E. Castaño[1,2], G. G. Mandayo[1,2]

[1]*CEIT & Tecnun, Donostia-San Sebastian, Spain*
[2]*CIC microGUNE, Arrasate-Mondragon, Spain*

**Abstract**

The aim of this work is to develop an easy-to-manufacture and highly-sensitive conductometric microsensor for indoor air quality (IAQ) monitoring. The sensing device consists on ZnO nanostructures on Pt interdigitated electrodes and a Pt heater surrounding the sensing layer, fabricated on one side of a 2.5x2.5 $mm^2$ alumina substrate. ZnO nanostructures are grown in-situ over the electrodes, using the Vapour-Solid (VS) approach. The samples were tested under different concentrations of benzene, formaldehyde, carbon monoxide and nitrogen dioxide, showing significant response to low concentrations of the four gases.


Peer-review under responsibility of the organizing committee of EUROSENSORS 2015

*Keywords:* VOC, ZnO, nanostructures, Vapour Solid, benzene, carbon monoxide, formaldehyde, nitrogen dioxide, indoor air quality

## 1. Introduction

Conductometric sensors using semiconductor oxides have been widely explored during the last years. The utilization of ZnO for gas sensors has a long history because of its chemical stability and sensitivity to different adsorbed gases, easiness to include additives, non-toxicity, and low cost. Systems mainly composed of ZnO have been studied as chemoresistive materials to detect gases like $H_2$, $NH_3$, $CH_4$, ethanol or CO, among others. The gas sensor response of zinc oxide conductometric sensors has been measured under several forms such as thin films [1-3], or nanostructures [4-6] of the material.

Nanostructures of semiconductor oxides [7] and in particular of ZnO [8,9] have been widely researched as candidates to promote detection due to their higher surface-to-volume ratio, which may also enhance diffusion processes and lead to a faster response of the sensor. The fabrication methods reported in the literature [10] are often based on thermal evaporation and chemical vapor deposition (CVD). This way, the nanostructures are grown over a


Peer-review under responsibility of the organizing committee of EUROSENSORS 2015
doi:10.1016/j.proeng.2015.08.768

substrate so their implementation over electrodes to get a conductometric sensor is usually difficult to achieve, because it frequently requires collecting the nanostructures and then depositing them over the sensing device. Therefore, the development of simple and reproducible routes to grow nanostructures localized on electrodes, such as the proposed here, is highly interesting in the way to develop fabrication methods applicable for mass production.

On the other hand, energy consumption in buildings accounts for the 40% of the global energy consumption [11]. The air intake minimization in order to reduce ventilation costs can reduce air quality, which is currently considered a public health problem [12]. Taking into account the results of the INDEX EU project [13], several compounds contribute to poor Indoor Air Quality (IAQ). In this paper, four of the compounds rated as first priority pollutants indoors will be tested: carbon monoxide, nitrogen dioxide, benzene and formaldehyde.

## 2. Experimental

The sensing devices are alumina chips of 2.5 mm x 2.5 mm fabricated on 0.5 mm-thick polished alumina substrates. The heater and the sensing element are Pt thin films patterned on the same side of the chip, and the heater surrounds the sensing area, which is a 0.5 mm x 0.5 mm square over the interdigitated electrodes. The heater and the interdigitated electrodes are 200 nm thick and were fabricated by DC sputtering in an Edwards ESM 100 system and shaped by lift-off process. The layout of the chip is described in [14].

Zinc layers were grown by sputtering and subsequently the Vapour Solid (VS) technique was used to get ZnO nanostructures in situ over the Pt electrodes, using a controlled oxygen flow. Zn was deposited by DC sputtering (Pfeiffer-Iontech classic 500) using a 4 diameter Zn target. Then, the samples were introduced in a tube furnace (PEO 601 from ATV) for annealing. As temperature is increased in nitrogen atmosphere, the zinc film is melted and evaporated. Then, the temperature is kept constant at the maximum for 2 hours and then it is decreased again in nitrogen. During the time oxygen enters the furnace at a low concentration, the zinc particles are oxidized forming ZnO nanoparticles and when the temperature decreases, these are deposited on the alumina substrate. Thus, nanostructures with different shapes can be obtained, as Fig. 1 summarizes.

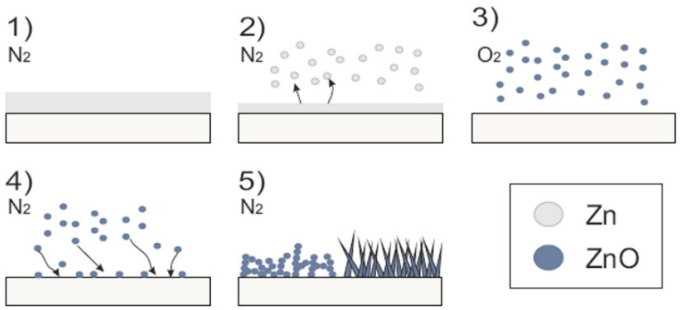


Fig. 1. Steps of Vapor-Solid technique for ZnO nanostructure growth.

Key parameters have been varied during the annealing treatment to study their influence on the NW growth: annealing temperature was changed from 500 to 700ºC, oxygen flow was varied between 55 and 220 sccm in a nitrogen flow of 2900 sccm and different thicknesses of Zn from 1 μm to 3.4 μm were deposited. Once the optimum values of these parameters were determined the NWs were grown over the electrodes.

The crystalline structure of the ZnO has been characterized by X-Ray diffraction using a Philips XPERT MRD diffractometer (Cu Ka1λ= 1.54059 Å). Additionally, a field emission gun scanning electron microscope (JEOL model JSM-7000F) has been used to analyze their morphology and microstructure.

The electrical response characterization of the sensors is carried out inside a sealed stainless steel chamber. The gas mixture in the chamber is obtained by using a system consisting of a PC-controlled mass flow controllers (MFCs) Bronkhorst Hi-Tech. GPIB communication between the computer and the MFCs control unit and Keithley Multimeters is automatically operated by Labview© for data acquisition.

## 3. Results and discussion

### *3.1. Structural characterization results*

Depending on the Zn layer thickness, the oxygen concentration, the annealing temperature, and the substrate, different structures were obtained in-situ over the electrodes by VS technique, as can be observed in the SEM micrographs in Fig. 2. Two different morphologies were obtained first on plain alumina substrates of 2 $cm^2$ and then were reproduced on Pt electrodes over alumina covering an area of 0.25 $mm^2$. Scanning Electron Microscope was used to analyze the sensing layers' morphology on both substrates. Depending on the ZnO growth conditions, nanobead-chain shape and nanoneedle shape structures were obtained. The growth conditions used for each substrate are summarized in Table 1.

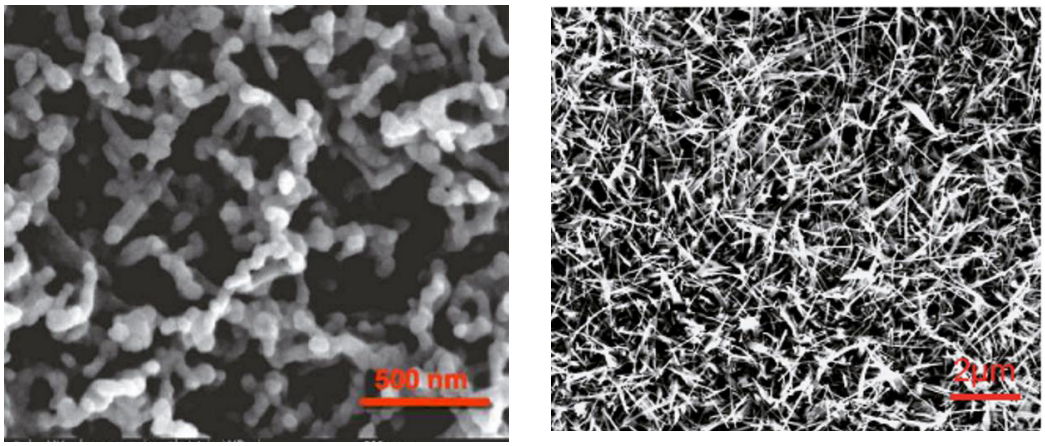


Fig. 2. SEM Micrograph of ZnO nanobead-chain (left) shape and nanoneedle shape (right) nanostructures.

Table 1. Summary of growth parameters for ZnO nanostructures growth on plain alumina and Pt electrodes on alumina

| | Nanobead-chain | | Nanoneedle | |
|---|---|---|---|---|
| | Plain alumina | Pt electrodes on alumina | Plain alumina | Pt electrodes on alumina |
| **Zn thickness** | 800 nm | 1 µm | 1µm | 3.4µm |
| **Oxygen flow** | 110 sccm | 110 sccm | 110 sccm | 110 sccm |
| **Nitrogen flow** | 2900 sccm | 2900 sccm | 2900 sccm | 2900 sccm |
| **Annealing T** | 550 ◦C | 550 ◦C | 550 ◦C | 650 ◦C |

As a general conclusion, thicker films are needed to get similar structures on Pt electrodes. This may be due not only to the need to cover the Pt step of 200 nm, but also to the necessity of a greater amount of Zn, as the area used on Pt electrodes is smaller than the area used on plain alumina. The need to increase temperature to get nanoneedles on Pt electrodes can also be caused by the greater thickness of material that needs to be evaporated in this case.

Both nanostructures' structural morphology has been studied using X-Ray diffraction. As can be observed in Fig.3, both nanostructures present a hexagonal ZnO structure [9], which is the structure of the mineral called zincite (peaks 1 to 11 in the graph). The absence of Zn peaks reveals that the zinc layer has been completely oxidized during the annealing process.

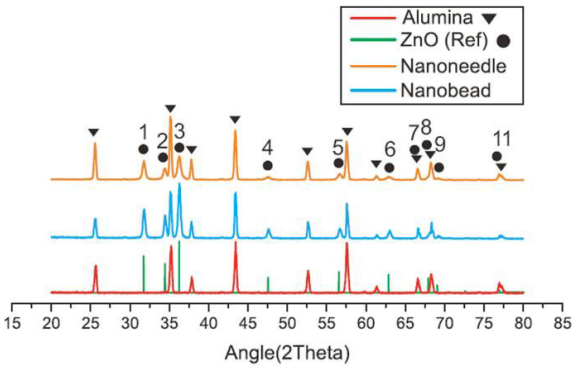


Fig. 3. Influence of Zn thickness on ZnO nanostructure diffraction patterns.

### *3.2. Electrical characterization results*

Both types of nanostructures were exposed to the four target gases, reaching ppb levels for benzene, formaldehyde and nitrogen dioxide. Here the ZnO nanoneedles response at different temperatures is reported (Fig. 4-left).

The sensor response to benzene at temperatures between 235◦C and 320◦C was studied. It was found that the optimal temperature for both the sensor response and response and recovery times is 310◦C. At this temperature the sensor exhibits a change of 36.1% to 5ppm of benzene, a response time of 4 minutes and a recovery time of 2.5 minutes. It is also observed that at temperatures lower than 280◦C the sensor needs a longer time to respond to the target gas and also to recover the baseline. At 235◦C , the sensor seems not to be reacting with the gas.

The same experiment for 5 ppm of formaldehyde was repeated in the same range of temperatures. The maximum response and the best response and recovery times are achieved working at 310◦C (as for benzene) and the obtained values are 24.8% for the response, 1 minute and 30 seconds for the response and recovery times respectively. It is also observed that the sensor does not react correctly at temperatures lower than 265◦C.

Regarding nitrogen dioxide, it was tested in the same temperature range and using the same concentration of 5 ppm. In this case, the maximum response was obtained at 195◦C, the lowest temperature in the measured range. Even having the maximum response at 195◦C, the sensor needs more time to react with the target gas and recover its baseline resistance value. When temperature is increased, the response value decreases but the reaction and recovery are faster.

Finally, the sensor was exposed to 30 ppm pulses of carbon monoxide working between 165 and 330◦C. The graph also shows that the sensor exhibits the highest response and the shortest response and recovery times at 330◦C.

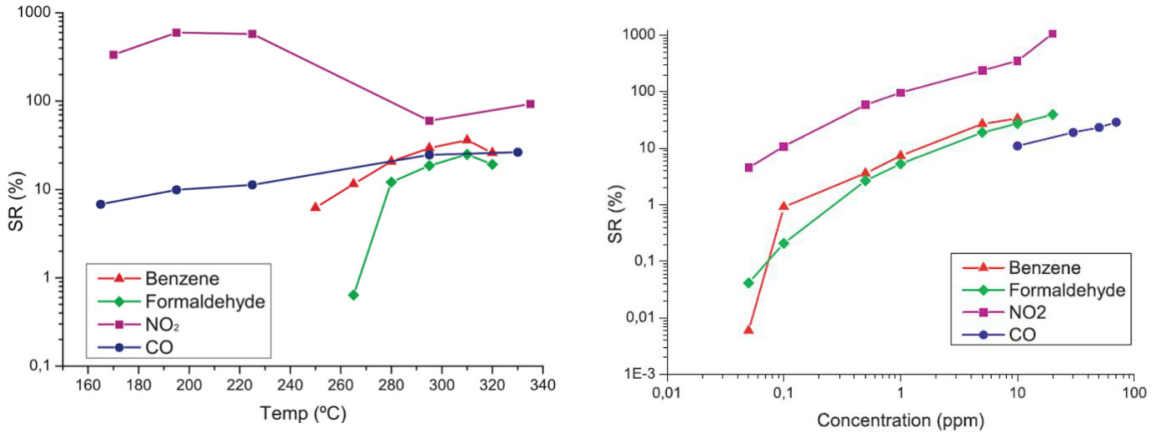


Fig. 4. ZnO nanoneedle based sensor response to 30 ppm of carbon monoxide and 5 ppm of benzene, formaldenhyde and nitrogen dioxide at different temperatures (left) and sensitivity curves for benzene, formaldehyde, carbon monoxide and nitrogen dioxide (right).

As a summary, the optimal temperature for $NO_2$ detection is 195◦C, while for formaldehyde and benzene is 310◦C. At 310◦C the sensor shows a change in resistance of 36.1%, 24.8% and 604% for benzene, formaldehyde and $NO_2$ respectively. In Figure 4-right, the sensor sensitivity curves within the tested ranges at each sensors' optimal temperature are shown.

Finally, Figure 6 shows the dynamic responses for the four target gases at the optimum working temperatures. The lowest detection limits achieved for these gases are 100 ppb for the benzene and formaldehyde, 50 ppb for nitrogen dioxide and 10 ppm for carbon monoxide, as low as the OSHA required action levels for IAQ.

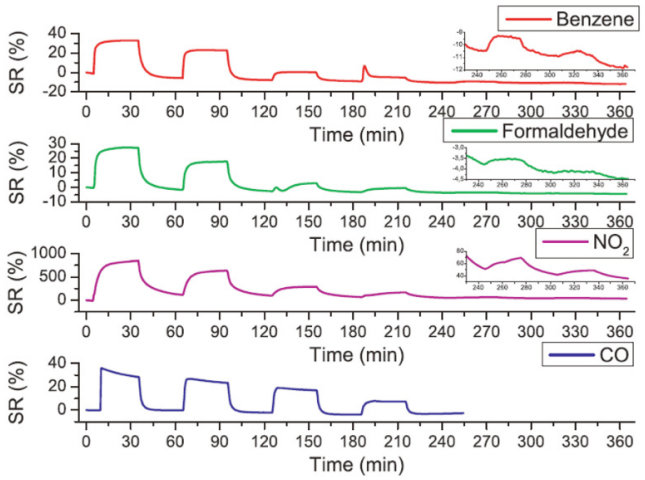


Fig. 5. Sensor dynamic response to pulses of 10, 5, 1, 0.5, 0.1 and 0.05 ppm of benzene, formaldehyde and nitrogen dioxide and 70, 50, 30 and 10 ppm of carbon monoxide working at its optimal temperature for each target.

## 4. Conclusions

ZnO nanoneedle based sensors show a sensitivity of 6.85%/ppm to benzene, 3.85%/ppm to formaldehyde, 46.14%/ppm to nitrogen dioxide and 0.3%/ppm to carbon monoxide at operating temperatures of 310, 310, 240 and

330◦C respectively. Detection limits below the OSHA actuation levels were reached: 100 ppb for benzene and formaldehyde, 50 ppb for nitrogen dioxide and below 10 ppm for carbon monoxide. Sensor response times ($t_{90}$) of 2 minutes for benzene, 8 minutes for formadeldehyde, 1 minute for $NO_2$ and carbon monoxide were measured for PELs. The results show that the developed material is susceptible to be used as gas sensor for indoor air quality. Table 2 summarizes the sensing properties of the nanoneedle-based sensor for each gas.

Table 2. Sensor detection limit, sensitivity and response and recovery time values for benzene, formaldehyde, carbon monoxide and nitrogen dioxide.

| | STEL[(1)] (ppm) | PEL[(2)] (ppm) | LOD[(3)] (ppb) | Sensitivity (%/ppm) | PEL response time (min) | 10 ppm response time (min) |
|---|---|---|---|---|---|---|
| **Benzene** | 2.5 | 1 | 100 | 6.65 | 2 | 1 |
| **Formaldehyde** | 0.75 | 0.75 | 100 | 3.85 | 8 | 3.5 |
| **Nitrogen dioxide** | 5 | 5 | 50 | 46.14 | 1 | 2 |
| **Carbon monoxide** | - | 50 | <10 ppm | 0.3 | 1 | 3 |

(1) Short Term Exposure Level Established by ACGIH
(2) Permissible Exposure Level Established by OSHA
(3) Limit of Detection

## Acknowledgements

Funding for this work was provided by the European Union through the INTASENSE project, grant no. 285037 “Integrated air quality sensor for energy efficient environment control" and by the Ministry of Economy and Competitiveness (MINECO) through the TEMIN-AIR project no. TEC2013-48147-C6-3-R “Technological innovation in micro and nanosensors for air quality monitoring and environmental control”.

## References

[1] A. Chatterjee, P. Mitra, and A. K. Mukhopadhyay. Chemically deposited zinc oxide thin film gas sensor. Journal of materials science, 34(17):4225–4231, 1999.
[2] X. Cheng, H. Zhao, L. Huo, S. Gao, and J. Zhao. ZnO nanoparticulate thin film: preparation, characterization and gas-sensing property. Sensors and Actuators B: Chemical, 102(2):248–252, 2004.
[3] H. Gong, J. Hu, J. Wang, C. Ong, and F. Zhu. Nano-crystalline Cu-doped ZnO thin film gas sensor for CO. Sensors and Actuators B: Chemical, 115(1):247–251, 2006a.
[4] P.-S. Cho, K.-W. Kim, and J.-H. Lee. NO2 sensing characteristics of ZnO nanorods prepared by hydrothermal method. Journal of electroceramics, 17(2-4):975–978, 2006.
[5] L. Liao, H. Lu, J. Li, H. He, D. Wang, D. Fu, C. Liu, and W. Zhang. Size dependence of gas sensitivity of ZnO nanorods. The Journal of Physical Chemistry C, 111(5): 1900–1903, 2007.
[6] C. S. Rout, S. Hari Krishna, S. Vivekchand, A. Govindaraj, and C. Rao. Hydrogen and ethanol sensors based on ZnO nanorods, nanowires and nanotubes. Chemical Physics Letters, 418(4):586–590, 2006.
[7] G. Cao and Y. Wang. Nanostructures and Nanomaterials: Synthesis, Properties, and Applications. World scientific series in nanoscience and nanotechnology. World Scientific, 2011.
[8] L. Schmidt-Mende and J. L. MacManus-Driscoll, ZnO nanostructures, defects and devices, Materials Today, 10(5): 40-48, 2007.
[9] D. Zappa, E. Comini and G. Sberveglieri, Thermally oxidized zinc oxide nanowires for use as chemical sensors, Nanotechnology, 24, 2013.
[10] R. Kumar, O. Al-Dossary, G. Kumar, A. Umar, Zinc oxide nanostructures for $NO_2$ gas-sensor applications: a review, Nano-Micro Letters 7(2):97-120, 2015.
[11] http://www.unep.org/sbci/AboutSBCI/Background.asp
[12] J. Sundell et al., Ventilation rates and health: multidisciplinary review of the scientific literature, Indoor Air 21(3), 2011.
[13] K. Koistinen et al., The INDEX project: executive summary of a EU project on indoor air pollutants, Allergy 2008: 63, 2008.
[14] J. González-Chavarri, I. Castro-Hurtado, I. Ayerdi, E.Castaño, G.G. Mandayo, ZnO conductometric sensor for indoor air quality measurement inside buildings, Proceedings of the 10th Spanish Conference on Electron Devices (CDE 2015), 11-13 February 2015, Aranjuez - Madrid, Spain, ISBN:9781479981090.